Journal of Chromatography, 628 (1993) 37–47
Elsevier Science Publishers B.V., Amsterdam

CHROM. 24 611

Analysis of alkylpyrrole autoxidation products by high-performance liquid chromatography with thermospray mass spectrometry and UV photodiode-array detection*

Mingshe Zhu and David C. Spink

Department of Environmental Health and Toxicology, The University at Albany, State University of New York; and Wadsworth Center for Laboratories and Research, New York State Department of Health, Albany, P.O. Box 509, NY 12201-0509 (USA)

Shelton Bank and Xi Chen

Department of Chemistry, The University at Albany, State University of New York, Albany, NY 12222 (USA)

Anthony P. DeCaprio

Department of Environmental Health and Toxicology, The University at Albany, State University of New York; and Wadsworth Center for Laboratories and Research, New York State Department of Health, P.O. Box 509, Albany, NY 12201-0509 (USA)

(First received June 19th, 1992; revised manuscript received September 3rd, 1992)

ABSTRACT

A method employing high-performance liquid chromatography with thermospray mass spectrometry (TSP-MS) and photodiode-array detection was developed and applied to the analysis of autoxidation products of 2,5-dimethyl-N-alkylpyrroles in aqueous solution under air or $^{18}O_2$. Numerous oxidation products were separated, characterized and categorized, primarily as (1) non-polar oligomers without incorporated oxygen, and (2) polar, oxygen-containing monomers. Kinetic studies showed that oligomerization was the dominant autoxidation pathway, with production of unstable dimers and trimers and, ultimately, a high-molecular-mass sediment. TSP-MS together with UV and proton nuclear magnetic resonance spectral data revealed that both the dimer and trimer contained a novel methylene bridge. These results suggest that this method is suitable for the analysis of alkylpyrrole autoxidation products that may be relevant to hexane neuropathy and products that are responsible for the instability of fuels in storage.

INTRODUCTION

Autoxidation of alkyl-substituted pyrroles is a phenomenon with important toxicological and chemical implications. For example, 2,5-hexanedione (2,5-HD), the ultimate neurotoxic γ-diketone metabolite of *n*-hexane, reacts with amino groups in neurofilament proteins to yield 2,5-dimethylpyrrole protein adducts [1]. These adducts undergo autoxidation, resulting in protein cross-linking *in vitro* [2,3] and *in vivo* [1,4]. Several groups have confirmed pyrrole formation as a necessary step in the pathogenesis of hexane neuropathy [5–7], although it is not clear whether autoxidative protein cross-linking is also required. One study indirectly showed that intermolecular cross-linking of protein required pyrrole adducts on both proteins, suggest-

Correspondence to: D. C. Spink, Wadsworth Center for Laboratories and Research, New York State Department of Health, P.O. Box 509, Albany, NY 12201-0509 (USA).

* Portions of this work were presented at the *40th ASMS Conference on Mass Spectrometry and Allied Topics, Washington, DC, May 31–June 5, 1992.*

0021-9673/93/$06.00

ing pyrrole-to-pyrrole bridging [8]. These reactions were accelerated by free radical initiators and thus were suggested to be free radical-mediated. In contrast, a recent investigation suggested that protein cross-linking was the consequence of the attack of a nucleophile such as a thiol or an amine of one protein on an electrophilic, oxidized pyrrole adduct of a second protein [9].

Alkylpyrrole autoxidation has also been associated with problems of storage instability of fossil and synthetic fuels. The presence of trace amounts of alkylpyrroles in these fuels under air atmosphere resulted in formation of a highly colored sediment [10–12]. 2,5-Dimethylpyrrole (DMP) was much more reactive than unsubstituted pyrrole and was used as a model compound in these experiments. Although several groups have presented evidence for the presence of different functional groups in the sediment produced in DMP oxidation [13,14] and have proposed reaction mechanisms [11,15], no intermediates or products of autoxidation have been identified.

It is well known that alkylpyrroles in aqueous or organic solutions are quickly oxidized by molecular oxygen to form insoluble, amorphous, and dark-colored polymers referred to as "pyrrole black" [16–18]. However, little structural information about these products is available. Alkylpyrrole oxidation products, particularly oligomers, are very difficult to analyze because they are extremely insoluble in water and in most organic solvents, and the intermediates in their formation appear to be very unstable.

Most previous attempts to analyze alkylpyrrole oxidation products have employed open column liquid chromatography and traditional chemical separation procedures such as extraction and distillation to isolate the oxidation products, followed by nuclear magnetic resonance (NMR) and infrared spectrometric analyses [17–19]. The instability of the autoxidation products during these manipulations renders several of these techniques inappropriate for their analysis. In addition, attempts to separate and analyze products of DMP autoxidation in dodecane and hexane by capillary gas chromatography (GC) have been unsuccessful [20], possibly because of the lack of volatility or the thermolabile nature of the products.

Reversed-phase high-performance liquid chromatography (HPLC) has been used successfully for the separation of several classes of pyrrole-containing compounds, including bile pigments [21] and phenylpyrrole derivatives that are products of tryptophan metabolism [22]. Coupling of HPLC with thermospray mass spectrometry (TSP-MS) [23,24] and with photodiode-array detection (PAD) [25] has proven useful for identification of unknown xenobiotic metabolites. This paper reports a method employing HPLC with TSP-MS and PAD for the separation and characterization of alkylpyrrole autoxidation products. In addition, we describe the structure of novel alkylpyrrole oligomers produced from 2,5-dimethyl-N-alkylpyrrole autoxidation.

EXPERIMENTAL

Materials

Ethanolamine and acetonitrile were obtained from Fisher Scientific (Fair Lawn, NJ, USA), and 5-amino-1-pentanol was obtained from Aldrich (Milwaukee, WI, USA). 2,5-Hexanedione was obtained from Eastman Kodak (Rochester, NY, USA). An equimolar mixture of $^{16}O_2$ and $^{18}O_2$, and [^{2}H]$CHCl_3$ were from Cambridge Isotope Labs. (Woburn, MA, USA). Water was purified by the Milli-Q system (Millipore, Bedford, MA, USA).

Synthetic procedures

Synthesis of 1-(2-hydroxyethyl)-2,5-dimethylpyrrole (HEDMP) was by Paal–Knorr condensation [26]. A mixture of ethanolamine (1 ml) and 2,5-HD (1 ml) was heated at 50°C under argon atmosphere for 1 h, followed by evaporation in vacuum (5 mmHg; 1 mmHg = 133.322 Pa) at 70°C for 2 h. A single component for the product was detected by HPLC and GC–MS, and its structure was confirmed as HEDMP by GC–MS (*m/z* 139, 108, 94), proton magnetic resonance (^{1}H NMR) spectroscopy (2.25 ppm, s. 6 H; 3.70 ppm, t. ^3J = 6 Hz, 2 H; 3.88 ppm, t. ^3J = 6 Hz, 2 H; 5.78 ppm, s. 2 H.) and UV spectroscopy (λ_{max} = 230 nm). 1-(2-Hydroxypentyl)-2,5-dimethylpyrrole (HPDMP) was prepared by the same method as HEDMP. The structure of HPDMP was confirmed by its TSP mass spectrum ([M + H]$^+$ at *m/z* 182), and UV absorption spectrum (λ_{max} = 226 nm). The product showed a single peak by HPLC. Pyrroles were maintained under argon to avoid reactions prior to the oxidation experiments.

Autoxidation of alkylpyrroles

Solutions of 1% (v/v) HEDMP in 0.2 *M* sodium phosphate buffer (pH 7.4) or 5% (v/v) phosphate buffer–methanol (90:5) were incubated at 37°C, in the dark, under air or $^{18}O_2$. Oxidation of HPDMP (5%, v/v) in phosphate buffer–methanol (1:1) was carried out under the same conditions. Each sample was filtered through a 0.2-μm nylon filter before analysis by HPLC.

HPLC–TSP-MS

The HPLC system (Waters, Milford, MA, USA) consisted of two Model 510 pumps, a Model 680 gradient controller, a Model 740 data module, a Model 490 multiwavelength detector and a Nova-Pak (Waters) C_{18} column (15 × 0.39 cm, 4-μm particle size). The TSP-MS system consisted of a Hewlett-Packard (Palo Alto, CA, USA) 5970 quadrupole mass analyzer and a Vestec (Houston, TX, USA) Model 101 thermospray interface. The data system consisted of a Hewlett-Packard series 200 computer with MS ChemStation software.

Chromatography was performed with gradients of acetonitrile concentration that were formed by pumping varying amounts of eluent A (0.1 *M* ammonium acetate in water) and eluent B (acetonitrile–water, 1:1, v/v, containing 0.1 *M* ammonium acetate) to give a total flow-rate of 1.2 ml/min. For the analysis of HEDMP oxidation samples the gradient was as follows: from 2% B to 20% B over 10 min, a hold for 15 min, to 70% B over 20 min, a hold for 5 min, to 100% B over 5 min, a hold for 5 min, to 2% B over 5 min. For the analysis of HPDMP oxidation samples the following gradient was used: from 20% to 40% B over 5 min, to 100% B over 20 min, a hold for 15 min, to 20% B over 5 min. The UV detector monitored two wavelengths, 225 and 320 nm, in the maxplot mode, which records the greater of the two absorbance values.

TSP-MS was performed with a source block temperature of 300–305°C, without the use of filament or discharge ionization. The vaporizer temperatures were chosen to be 10°C below the total vaporization point of the initial mobile phase. The vaporizer setting was sufficiently low to prevent fluctuations in ionization as the mobile phase composition changed later in the gradient.

HPLC–PAD detection

The Waters HPLC–PAD system consisted of two 6000A solvent delivery pumps, a WISP 710B sample processor, a Model 720 controller, and a Model 990 photodiode-array detector. The columns, mobile phases, and gradients used for the separation of pyrrole oxidation products were same as those used in the HPLC–TSP-MS analyses, except that the flow-rate was 1.4 ml/min. UV absorbance spectra were recorded over the range of 200 to 400 nm with a 2-s scanning interval.

GC–MS

The GC–MS system (Hewlett-Packard) consisted of a Model 5890 GC, a Model 5970 quadrupole mass analyzer and a Model 9000 computer with MS ChemStation software. A fused-silica capillary column (HP-1, 12 m × 0.2 mm, Hewlett-Packard) was used with helium as the carrier gas at a head pressure of 30 kPa.

^1H NMR spectroscopy

The HPLC peak corresponding to HEDMP dimer was collected and immediately subjected to nitrogen sparging. The eluted sample was then lyophilized and redissolved in 0.5 ml $[^2H]CHCl_3$ and placed in a 5-mm NMR tube maintained at room temperature. ^1H NMR spectra were acquired on a Varian XL-300 multinuclear spectrometer operating at 299.94 MHz using a 4000 Hz sweep width and 16 000 data points. The pulse width was set as 5.0 μs to provide a 30° flip angle. The recycle time was 2.0 s. A desirable signal-to-noise ratio was obtained after 1000 transients were acquired. Chemical shifts were referenced to tetramethylsilane (TMS).

Methods for kinetic and stability studies

Freshly synthesized HEDMP was added to phosphate buffer to give a 1% (v/v) solution and allowed to autoxidize at 37°C in the dark under air atmosphere. Aliquots of this solution were analyzed by HPLC after 3, 18, 72 and 122 h of oxidation. In order to test the stability of autoxidation products in aqueous solution, major products of HEDMP autoxidation (5%, v/v, 5-day sample) were isolated by HPLC and lyophilization. These were redissolved in phosphate buffer (1:5 dilution compared with original oxidation solution) and reincubated

under the same autoxidation conditions. Concentrations of the major components at different periods of incubation were determined by HPLC.

RESULTS AND DISCUSSION

HPLC separation of pyrrole autoxidation products

The spontaneous autoxidation of HEDMP in aqueous solution yielded a complex mixture of products which are illustrated in a three-dimensional HPLC–PAD plot (Fig. 1). Peak A5, corresponding to HEDMP, exhibited a UV absorbance maximum at 230 nm. Other peaks represented autoxidation products, some of which (peaks A1 and A2) showed absorbance maxima in the range of 310 to 340 nm. Based on these UV spectral data, 225 and 320 nm were chosen as HPLC multiple detection wavelengths in order to simultaneously detect parent pyrroles and their major oxidation products. Fig. 2a shows a dual-wavelength HPLC chromatogram of HEDMP after incubation in phosphate buffer (5%, v/v) under air atmosphere for 174 h. Autoxidation products of HEDMP were also detected by on-line TSP-MS. Fig. 2b shows the total ion current (TIC) chromatogram recorded during the same sample analysis (10-fold greater sample injection) as in Fig. 2a. Both detection methods showed a similar pattern of oxidation products. The lower relative response in the TIC chromatogram to components eluting later in the gradient (*e.g.*, peak A7) reflects the suppressive influence of acetonitrile on the ionization.

Reversed-phase HPLC of HPDMP autoxidation products in aqueous solution and of a $CHCl_3$ extract of "pyrrole black" are presented in Fig. 3, in which peak B3 represents HPDMP. HPLC elution profiles of both HEDMP (Fig. 2) and HPDMP (Fig. 3) oxidation samples showed similar patterns for major autoxidation products. Several polar products (peak A1, A2 and A3 in Fig. 2a and peak B1 and B2 in Fig. 3) eluted at low concentrations of acetonitrile, and two non-polar products (peaks A6 and A7 in Fig. 2a and peaks B4 and B5 in Fig. 3) were found to be concentrated in the $CHCl_3$ extract.

A single analysis by HPLC on C_{18} columns enabled the separation of numerous components, including polar, oxygen-containing monomers and unstable oligomers (see below). In contrast, GC–MS was found to be inappropriate for the analysis of the pyrrole derivatives in these complex mixtures (data not shown). The advantages of this HPLC method include the lack of a requirement for chemical derivatization or other sample pretreatment, and increased sensitivity and rapidity of analysis as compared with previously used open column chro-

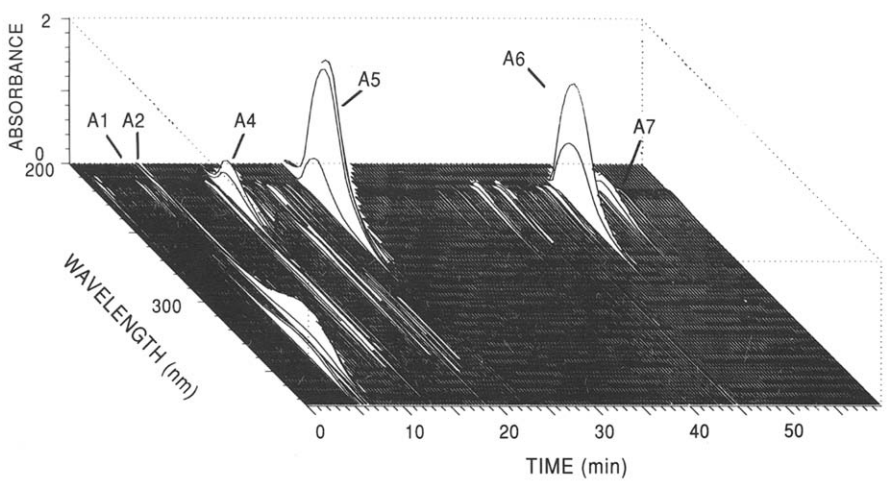

Fig. 1. Three-dimensional HPLC–PAD chromatogram from the analysis of an HEDMP autoxidation sample. HEDMP was incubated in phosphate buffer (5%, v/v) under air for 89 h (see under Experimental). Peak A5 corresponds to HEDMP; other peaks represent autoxidation products.

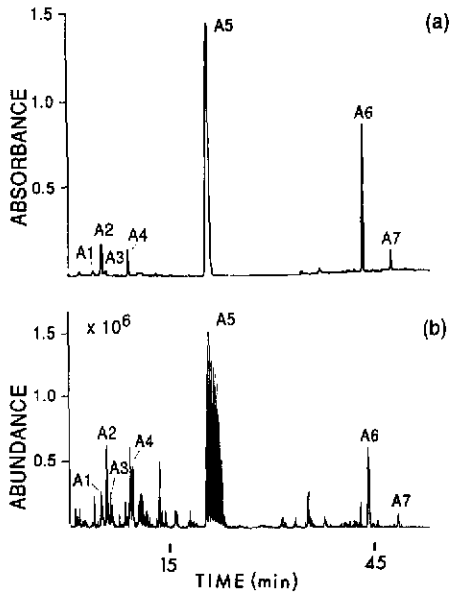

Fig. 2. HPLC separation of HEDMP autoxidation products. HEDMP was incubated in phosphate buffer (5%, v/v) under air for 174 h. (a) Maxplot chromatogram (dual-wavelength detection; 225 and 320 nm). (b) Total ion current chromatogram from HPLC–TSP-MS analysis of the same sample. Peak designations refer to data in Table I.

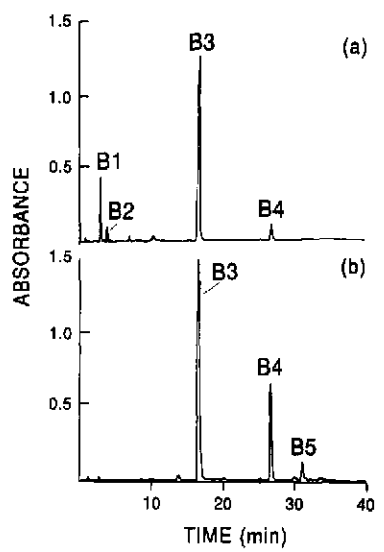

Fig. 3. HPLC separation of HPDMP autoxidation products. HPDMP was incubated under air for 76 h (see under Experimental). (a) Maxplot chromatogram (225, 320 nm) of HPDMP oxidation solution. (b) Maxplot chromatogram of $CHCl_3$ extract from autoxidation sediment. Peak B3 represents HPDMP, while other peaks correspond to its oxidation products.

matographic techniques. In addition, the HPLC technique has the capability of quantitative determination, providing a useful tool for kinetic studies of alkylpyrrole autoxidation.

Characterization of autoxidation products by TSP-MS and PAD

Thermospray mass spectra of both parent pyrroles exhibited single peaks representing protonated molecules without fragmentation (Figs. 4a and 5a). TSP mass spectra of major products of both HEDMP and HPDMP autoxidations are summarized in Table I. To investigate the incorporation of oxygen into alkylpyrrole autoxidation products, HEDMP was oxidized under an equimolar of mixture of $^{16}O_2$ and $^{18}O_2$. TSP mass spectra of these autoxidation products were recorded and are summarized in Table I. In addition, PAD was employed

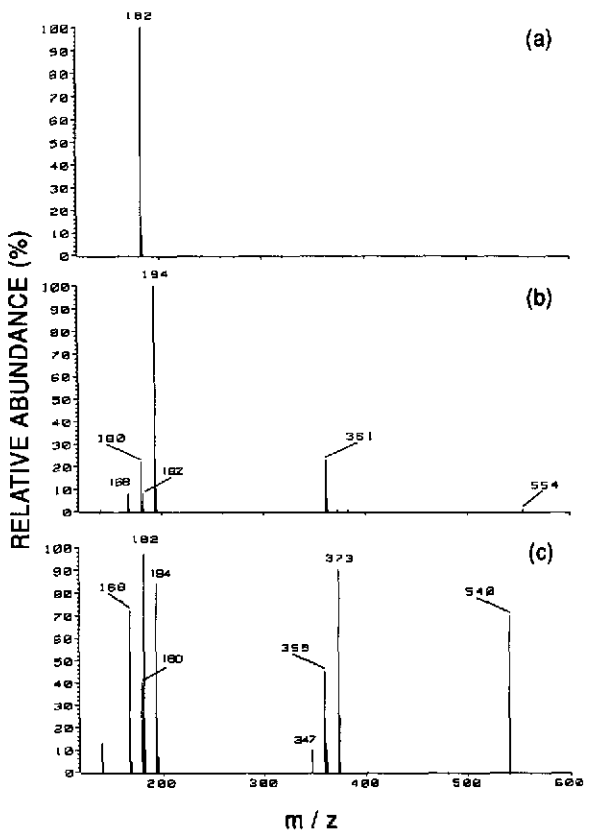

Fig. 4. Representative TSP mass spectra of HPDMP and its oligomers. (a) HPDMP; (b) HPDMP dimer; (c) HPDMP trimer. Molecular ions, major fragments and HPLC retention times are listed in Table I.

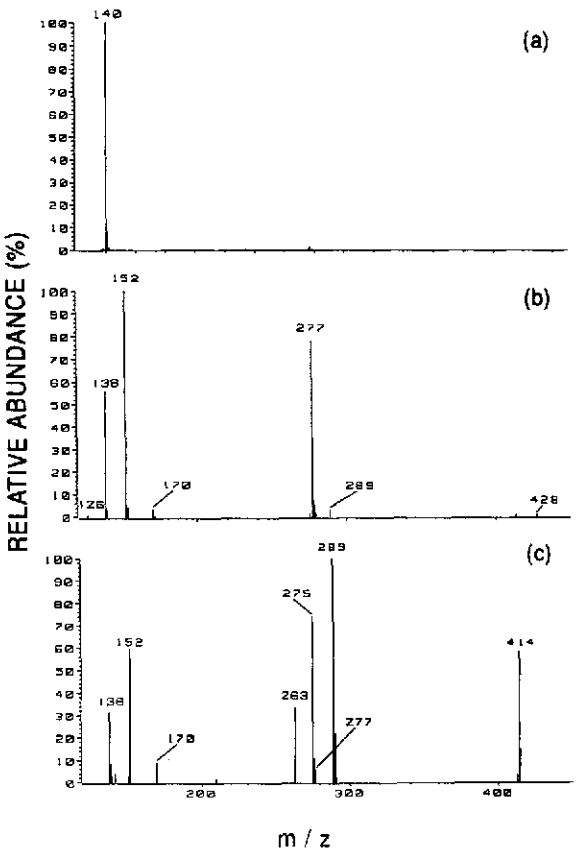

Fig. 5. Representative TSP mass spectra of HEDMP and its oligomers. (a) HEDMP; (b) HPDMP dimer; (c) HEDMP trimer. Molecular ions, major fragments and HPLC retention times are listed in Table I.

to provide structural information (Table I), since the substitution of carbonyl or other groups containing double bonds at the pyrrole methyl carbon, and/or the coupling of a pyrrole ring directly to that of the second pyrrole would be expected to extend the conjugation of the system, resulting in absorbance at longer wavelengths [27,28].

As can be seen in the UV chromatogram, one major group of autoxidation products consisted of non-polar alkylpyrrole species (peaks A6 and A7 in Fig. 2 and peaks B4 and B5 in Fig. 3). TSP mass spectra of the two non-polar oxidation derivatives of HPDMP are shown in Fig. 4b and 4c. On the basis of intense ions corresponding to $[M + H]^+$, peaks B4 and B5 were assigned to the dimer and trimer of HPDMP, respectively. Similarly, two non-polar products of HEDMP autoxidation were determined to be the dimer (Fig. 5b) and trimer of HEDMP (Fig. 5c).

Another major category of autoxidation products was polar oxygen-containing alkylpyrrole monomers. Two components eluting from the HEDMP autoxidation solution (peaks A1 and A2 in Fig. 2a) exhibited the same molecular ion $[M + H]^+$ at m/z 172, corresponding to the mass of the protonated alkylpyrrole plus 32 (Table I). The data suggested incorporation of two oxygen atoms, possibly due to sequential oxidation of the pyrrole methyl group to an aldehyde and then to a carboxylic acid. In addition, a common fragment ion (m/z 154) of both components may have resulted from the loss of water from the $[M + H]^+$ ion. TSP-MS of these two products (Table I) following autoxidation under a 1:1 mixture of $^{16}O_2$ and $^{18}O_2$ showed similar intensities of peaks at m/z 172 and 174 and ions assigned to $[M + H - H_2O]^+$ at m/z 154 and 156, but no isotopic peak at m/z 176. These data indicated that during the oxidation process only one oxygen atom was incorporated into alkylpyrrole from molecular oxygen, which remained in the alkylpyrrole fragment after the loss of water during thermospray ionization. The second oxygen atom was probably incorporated from the aqueous solvent.

The values of λ_{max} of these derivatives, 338 nm for peak A1 and 328 nm for peak A2, were consistent with extended conjugation of the pyrrole ring with functional groups that contain a double bond, possibly resulting from oxidation of the pyrrole methyl groups to aldehydes. For HPDMP autoxidation, similar monomeric autoxidation products (peaks B1 and B2) were present in UV chromatograms; these exhibited the same pattern of $[M + H]^+$ ions and value of λ_{max} (Table I). The component corresponding to peak A3 (Table I) was another monomeric HEDMP derivative that exhibited a $[M + H]^+$ ion consistent with incorporation of only one oxygen atom.

In addition to the two categories of major products, there were a number of minor autoxidation products from both alkylpyrroles (Figs. 2 and 3). These minor pyrrole derivatives exhibited moderate polarity and were observed only after prolonged in-

TABLE I

CHARACTERIZATION OF MAJOR PRODUCTS OF HEDMP AND HPDMP AUTOXIDATION

Peak[a]	Retention time (min)	TSP-mass spectra *m/z* (relative intensity)	λ_{max}
A1	4.8	172[b] (100), 154 (9) [174 (76), 172 (100), 156 (28), 154(35)][c]	338
A2	5.6	172[b] (100), 154 (32) [174 (100), 172 (92), 156 (54), 154(81)][c]	328
A3	6.1	156[b] (100), 154 (66) [158 (42), 156 (100), 154 (38)][c]	317
A4	8.9	170[b] (55), 152 (100)	224
A5	19.9	140[b] (100)	230
A6	42.9	428[d] (0.3), 289[d] (0.8), 277[b] (66), 152 (100), 140 (4), 138 (94), 126 (4)	229
A7	47.3	565[d] (0.1), 428[d] (2), 414[b] (24), 289 (67), 277 (9), 275 (79), 263 (17), 152 (100), 140 (15), 138 (89)	226
B1	2.9	214[b] (100), 196 (22)	337
B2	4.2	214[b] (21), 198 (100), 196 (42)	318
B3	18.1	182[b] (100)	226
B4	29.1	554[d] (0.8), 373[d] (0.5), 361[b] (24), 194 (100), 182 (8), 180 (22), 168 (8)	225
B5	33.9	540[b] (18), 373 (100), 359 (18), 347 (6), 194 (59), 182 (61), 180 (28),168 (50)	223

[a] Peaks A1–A7 are from the analysis of HEDMP autoxidation, peaks B1–B5 are from the analysis of HPDMP oxidation.
[b] Assigned to $[M + H]^+$;
[c] Oxidation under $^{16}O_2/^{18}O_2$;
[d] Assigned to adduct ion.

cubation time. Based on their respective $[M + H]^+$ ions, most of them were assigned as various oxygen-containing dimers. For example, in HEDMP oxidation samples, a peak at retention time 14 min exhibited an apparent $[M + H]^+$ at *m/z* 293, consistent with a dimer with one oxygen atom incorporated, while another peak (retention time 30.6 min) showed an apparent $[M + H]^+$ ion at *m/z* 311, corresponding to a dimer with two oxygens incorporated (Fig. 2).

Identification of the alkylpyrrole dimer

An important goal of this study was to characterize the type of linkage in 2,5-dimethyl-N-alkylpyrrole dimers and larger polymers, since it may constitute the protein cross-link in 2,5-HD-treated protein. The dimer molecular mass indicated by TSP-MS suggested oxidation, or a net loss of 2 H, in its formation. In addition, the identical UV spectra of alkylpyrrole monomer and dimer (Table I) indicated a lack of conjugation between the pyrrole

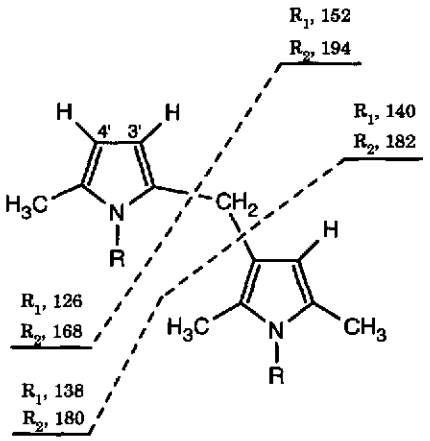

Fig. 6. Proposed general structure of 2,5-dimethyl-N-alkylpyrrole dimer and its thermospray mass spectral fragmentation pattern. R_1 is $-(CH_2)_2OH$ and R_2 is $-(CH_2)_5OH$.

rings of the dimer. These results argued against a direct ring-to-ring dimeric bridging structure [28], and were instead consistent with involvement of either the methyl or N-alkyl groups in pyrrole dimeric bridging. Since the only structural difference between the two pyrrole monomers examined in this study was in the N-alkyl group, the mass spectra would have exhibited some differences if the N-alkyl group was involved in cross-linking. This possibility was excluded by the identical fragmentation patterns of both HEDMP and HPDMP dimers.

Fig. 6 shows the proposed structure and TSP-MS fragmentations of the 2,5-dimethyl-N-alkylpyrrole dimers, which contain methylene bridges from C-2 of one pyrrole ring to C-3 of another pyrrole ring. During thermospray ionization, the N-alkylpyrrole moieties remained intact, while the methylene bridges were less stable. The TSP mass spectra of the dimers (Fig. 4b and Fig. 5b) showed peaks which were interpreted as being formed by cleavage of either of the C–C bonds of the methylene bridge (Fig. 6). Despite the fact that both fragments would be derived from substituted pyrroles and thus would be expected to have high proton affinities, in each case ions from the fragment retaining the methylene carbon, *e.g.* the ions with *m/z* 152 and 138 in the mass spectrum of the HEDMP dimer, showed much higher intensities than those derived from the other pyrrole ring, *e.g.* the ions with *m/z* 126 and 140. This might be explained by protonation of the dimer followed by a cleavage mechanism [29] in which the ions at *m/z* 138 and 152 arise from formation of alkyl-substituted 1- and 2-azafulvenium ions carrying the positive charge, and the second pyrrole is eliminated as a neutral fragment that would require subsequent protonation for MS detection.

In addition, there were several adduct ions with higher values of *m/z* than those of the corresponding $[M + H]^+$ ions in the mass spectra of both the HEDMP and the HPDMP dimers (Figs. 4b and 5b). The formation of these ions also followed a pattern. For example, the ion at *m/z* 428 in the mass spectrum of HEDMP dimer could be interpreted as an adduct of the dimer with a major fragment ion (*m/z* 152). This TSP mass fragmentation pattern may be characteristic of the unique bridge structure of 2,5-dimethyl-N-alkylpyrrole dimers and higher oligomers.

In the ^1H NMR spectrum of the HEDMP dimer (Fig. 7), three singlets were observed at 2.16, 2.18 and 2.24 ppm, respectively, which arise from three isolated methyl groups on the pyrrole ring (protons labeled e in the structure illustrated in Fig. 7). Four triplets, at 3.55, 3.74, 3.86 and 3.89 ppm, were as-

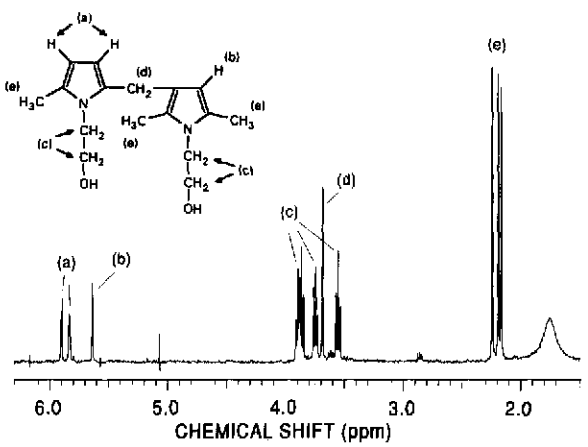

Fig. 7. The ^1H NMR spectrum of the HEDMP dimer. Chemical shifts were referenced to TMS. The numbers of protons within specified chemical shift ranges are: 2.1 to 2.3 ppm, 9; 3.5 to 3.6 ppm, 2; 3.6 to 3.8 ppm 4; 3.8 to 4.0 ppm, 4; 5.6 to 5.7 ppm, 1; 5.8 to 6.0 ppm, 2. The letters assigned to groups of peaks on the spectrum correspond to the letters denoting the different groups of protons in the proposed structure.

signed to the four methylenes in the two 2-hydroxyethyl groups (protons labeled c, ^3J = 5.0 Hz). A singlet at 3.68 ppm was assigned to the isolated methylene connecting the two pyrrole rings (protons labeled d). In the aromatic region, a singlet at 5.63 ppm was assigned to the isolated proton on one of the pyrrole rings (proton b), and the two doublets at 5.83 and 5.89 ppm were ascribed to the two vicinal protons on the second pyrrole ring (protons a, ^3J = 3.5 Hz). There were three non-equivalent methyl groups in the HEDMP dimer, as demonstrated by its ^{1}H NMR spectrum, implying that the dimerization was not symmetrical. Asymmetry of the dimer is also supported by the appearance of two pairs of triplets which arise from two chemically non-equivalent ethylene groups in the N-alkyl sidechains. The appearance of the aromatic proton signals indicate that one proton is isolated on one of the pyrrole rings and that the other two are adjacent on the second pyrrole ring. All these observations confirm the proposed methylene bridge structure of the HEDMP dimer as shown in Figs. 6 and 7.

UV spectral data also indicated that 2,5-dimethyl-N-alkylpyrrole trimers were formed without conjugation between the pyrrole rings. Furthermore, a similar TSP-MS fragmentation pattern of the trimer as with the dimer suggested an identical methylene bridging structure (Table I). This trimer is proposed to be formed by substitution at the C-4′ position of the dimer by a methyl carbon of a third pyrrole monomer (Fig. 6). Since there are two methylene-bridge linkages in this trimer, cleavage of the C–C bonds on either side of the methylene bridges could yield a total of eight fragment ions in the mass spectra of both HPDMP and HEDMP trimers. Most of these ions were observed (Figs. 4c, 5c and Table I). An isomer of the proposed trimer having the same linkage structure but a different substitution position (*i.e.* at C-3′ of the dimer; Fig. 6) is also possible. However, the structure of the trimer with C-4′ substitution is considered the most likely because it would have less steric hindrance.

Kinetic studies

The time course of HEDMP autoxidation is illustrated in Fig. 8. At 3 h (Fig. 8a), only the peak corresponding to the HEDMP dimer (peak A6) was present, indicating that this derivative was produced in the initial stage of autoxidation. After 18 h, the solution was slightly yellow, and HPLC at this time (Fig. 8b) revealed primarily dimer and

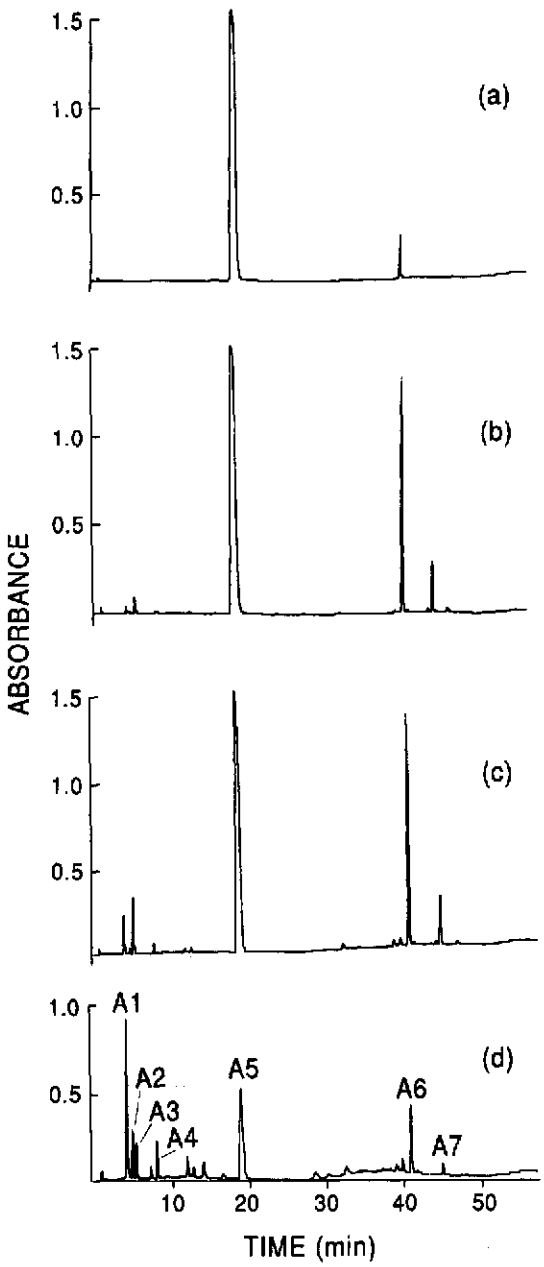

Fig. 8. Time course of HEDMP autoxidation. HEDMP was oxidized in phosphate buffer (1%, v/v) under air for various times. (a), (b), (c), (d) Analysis of samples after 3, 18, 44 and 128 h incubation, respectively. The oxidation products were analyzed by HPLC with dual-wavelength detection (maxplot; 225 and 320 nm).

trimer (peak A7), suggesting that the HEDMP dimer may further react with HEDMP monomer to form the trimer. In addition, two polar, oxygen-containing products (peaks A1 and A3) were present at much lower concentrations at this time. The concentrations of the dimer and the trimer in reaction solutions reached a maximum after 44 h of oxidation (Fig. 8c) and then slowly decreased. In contrast, the levels of oxygen-containing polar monomeric products increased proportionally with incubation time. The only exception was peak A3, corresponding to a monomer with one oxygen incorporated, which decreased in intensity during the middle period of autoxidation.

In the later stages of autoxidation (122 h), a "pyrrole black" sediment was present. HPLC at 122 h (Fig. 8d) revealed a decrease in the concentrations of the HEDMP monomer, dimer and trimer, while polar monomeric components were now the major products, in particular peak A1. Results of other studies with isolated component A2 suggest that A1 may have been generated from A2 during prolonged incubation. Additionally, HPLC analysis at 122 h showed a number of new peaks, possibly representing additional autoxidation products, such as oxygen-containing dimers (*e.g.* $[M + H]^+$ at m/z 309) or degradation products of the polymers.

Fig. 9 shows the stability of HEDMP dimer, trimer, and polar monomeric derivatives, recovered by HPLC and then reincubated in aqueous solution. Both oligomers were unstable, with $t_{1/2}$ of approximately 10–12 h. This indicated that these oligomers may quickly undergo further reactions to form polymers or other unknown insoluble products. Additionally, the decrease in the relative concentration of the HEDMP dimer with time followed apparent first-order kinetics. The instability of the dimer and trimer in aqueous solution accounts for the decrease in the concentrations of these derivatives in the later stages of autoxidation (Fig. 8). In contrast, the intensities of peak A4 and the total of peaks A1 and A2 were relatively constant in aqueous solution (Fig. 9). Studies of the time course of autoxidation and stabilities of the major products in aqueous solution revealed that the formation of pyrrole dimer was the predominant reaction at physiological pH. However, there were additional pathways yielding oxygen-containing monomers or other derivatives which occurred at a slower rate.

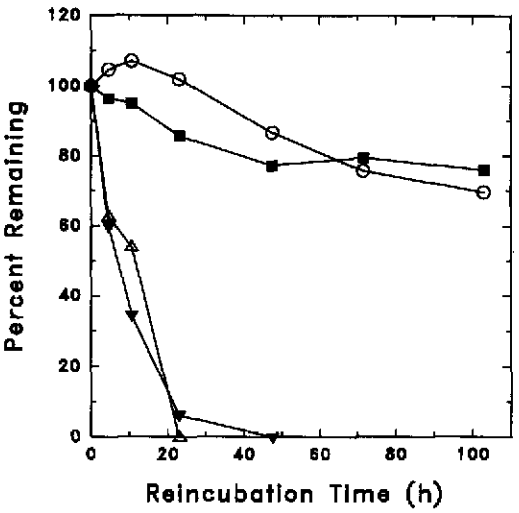

Fig. 9. Stability of major HEDMP autoxidation products in aqueous solution. Isolated HEDMP oxidation products (collected from HPLC eluent) were reincubated in phosphate buffer (*ca.* 1%, v/v). Relative levels of these components were measured as peak areas by HPLC maxplot with dual-wavelength detection after various reincubation times, as compared with zero time areas. Retention times, UV absorption data, and molecular mass information of individual components corresponding to each peak are listed in Table I. ■ = Peak A1 plus peak A2; ○ = peak A4; ▼ = peak A6; △ = peak A7.

CONCLUSIONS

The application of HPLC coupled with TSP-MS and PAD allowed the simultaneous separation and characterization of autoxidation products of 2,5-dimethyl-N-alkylpyrroles, including polar, oxygen-containing monomers and high-molecular-mass oligomers. The proposed methylene bridge structure formed upon dimerization of these pyrroles, which has not been previously reported, was confirmed by ^1H NMR spectroscopy. The techniques reported here should be useful in future mechanistic studies of pyrrole chemistry as it relates to hexane neurotoxicity and the stability of petroleum-based fuels.

ACKNOWLEDGEMENTS

This work was supported in part by a research grant (ES-05172) from the US National Institute for Environmental Health Sciences. In addition,

support from the National Science Foundation for the purchase of the NMR instrumentation used in this research is gratefully acknowledged.

REFERENCES

1 A. P. DeCaprio and E. A. O'Neill, *Toxicol. Appl. Pharmacol.*, 78 (1985) 235.
2 A. P. DeCaprio, E. J. Olajos, and P. Weber, *Toxicol. Appl. Pharmacol.*, 65 (1982) 440.
3 D. G. Graham, D. C. Anthony, K. Boekelheide, N. A. Maschmann, R. G. Richard, J. W. Wolfram and B. R. Shaw, *Toxicol. Appl. Pharmacol.*, 64 (1982) 415.
4 D. M. Lapadula, R. D. Irwin, E. Suwita and M. B. Abou-Donia, *J. Neurochem.*, 46 (1986) 1843.
5 L. M. Sayre, C. M. Shearson, T. Wongmongkolrit, R. Medori and P. Gambetti, *Toxicol. Appl. Pharmacol.*, 84 (1986) 36.
6 M. B. Genter, G. Szakal-Quin, C. W. Anderson, D. C. Anthony and D. G. Graham, *Toxicol. Appl. Pharmacol.*, 87 (1987) 351.
7 A. P. DeCaprio, R. G. Briggs, S. J. Jackowski and J. C. S. Kim, *Toxicol. Appl. Pharmacol.*, 92 (1988) 75.
8 A. P. DeCaprio, *Mol. Pharmacol.*, 30 (1986) 452.
9 D. C. Anthony, V. Amarnath and D. G. Graham, *Toxicologist*, 10 (1990) 183.
10 A. A. Oswald and F. Noel, *J. Chem. Eng. Data*, 6 (1961) 294.
11 J. Li and N. C. Li, *Fuel*, 64 (1985) 1041.
12 J. W. Frankenfeld and W. F. Taylor, *Ind. Eng. Chem. Prod. Res. Dev.*, 22 (1983) 615.
13 J. W. Frankenfeld and W. F. Taylor, *Ind. Eng. Chem. Prod. Res. Dev.*, 22 (1983) 608.
14 M. C. Loeffler and N. C. Li, *Fuel*, 64 (1985) 1047.
15 J. V. Cooney and R. N. Hazlett, *Heterocycles*, 22 (1984) 1513.
16 A. Gossauer and P. Nesvadba, in R. A. Jones (Editor), *Pyrroles, Part I, Synthesis and Physical and Chemical Aspects of the Pyrrole Ring*, Wiley, New York, 1990, p. 499.
17 E. Höft, A. R. Katritzky and M. R. Nesbit, *Tetrahedron Lett.*, 32 (1967) 3041.
18 E. B. Smith and H. B. Jensen, *J. Org. Chem.*, 32 (1967) 3330.
19 G. B. Quistad and D. A. Lightner, *Tetrahedron Lett.*, 46 (1971) 4417.
20 B. D. Beaver, J. V. Cooney and J. M. Watkins, Jr., *J. Heterocyclic Chem.*, 23 (1986) 1095.
21 G. B. Odell, W. S. Mogilevsky and G. R. Gourley, *J. Chromatogr.*, 529 (1990) 287.
22 N. E. Mahoney and J. N. Roitman, *J. Chromatogr.*, 508 (1990) 247.
23 J. K. Baker, R. H. Yarber, C. D. Hufford, I. Lee, H. N. El Sohly and J. D. McChesney, *Biomed. Environ. Mass Spectrom.*, 18 (1988) 337.
24 I. G. Beattie and T. J. A. Blake, *Biomed. Environ. Mass Spectrom.*, 18 (1989) 872.
25 R. L. Jansing, E. S. Chao and L. S. Kaminsky, *Mol. Pharmacol.*, 41 (1992) 209.
26 C. Paal, *Chem. Ber.*, 17 (1884) 2756.
27 A. I. Scott, *Interpretation of Ultraviolet Spectra of Natural Products*, Pergamon Press, New York, 1964, p.165.
28 L. Chierici and G. P. Gardini, *Tetrahedron*, 22 (1966) 53.
29 D. J. Chadwick, in R. A. Jones (Editor), *Pyrroles, Part I, Synthesis and Physical and Chemical Aspects of Pyrrole Ring*, Wiley, New York, 1990, p. 65.